Investigation on Address Discharge Characteristics for R, G, and B Cells and Effects of Phosphor Thickness on Address Discharge Delay in AC PDP

H. D. Park, H.-S. Tae, H.-S. Jeong*, M. Hur*, and M. Yoo*

School of Electrical Engineering and computer science, Kyungpook National University, Daegu, Korea

* R&D Team, PDP Division, Samsung SDI Co. Ltd, Korea

ABSTRACT

In this paper, the address discharge characteristics are analyzed in the red, green, and blue cells, respectively by using the V_t closed-curve method. To reduce the difference of the address discharge delay among the R, G, and B cells, the effects of the phosphor thickness on the address discharge delay are examined. By controlling properly the phosphor thickness among the R. G. and B cells, the difference of the address discharge delay is observed to be minimized among the R, G, and B cells.

1. INTRODUCTION

The stable address discharge is still essential for the low cost high image quality ac-plasma display panel. In particular, the stable address discharge delay characteristics irrespective of the R, G, and B cell difference is the most important factor for the realization of the high-speed address under wider dynamic driving margin in the AC-PDP with millions of micro-discharge cells [1, 2, 3, 4]. However, the firing voltages of the plate gap discharge are different mainly due to the R, G, and B cells, thus resulting in the unstable address discharge. In this study, the address discharge characteristics of the R, G, and B cells are analyzed and compared by using the V_t closed-curve analysis. In addition, to reduce the address discharge delay time difference among the R, G, and B cells, the address discharge characteristics are analyzed by varying the phosphor thicknesses of the R, G, and B cells.

2. EXPEREMENT SETUP

Figs. 1 (a) and (b) show the test panel structure and the schematic diagram of three electrodes in 50-in. full-HD PDP test panel employed in the current study. As shown in Fig. 1 (a), the test panel used in this work was a commercial 50-in. full HD PDP with a box-type barrier rib. The gas mixture and pressure of test panel were Ne-He-Xe(11%) and 420 Torr. The gap between the coplanar electrodes and the barrier rib height are fixed at 70 μm and 110 μm, respectively. As shown in Fig. 1 (b), the scan (Y) and common (X) electrodes are

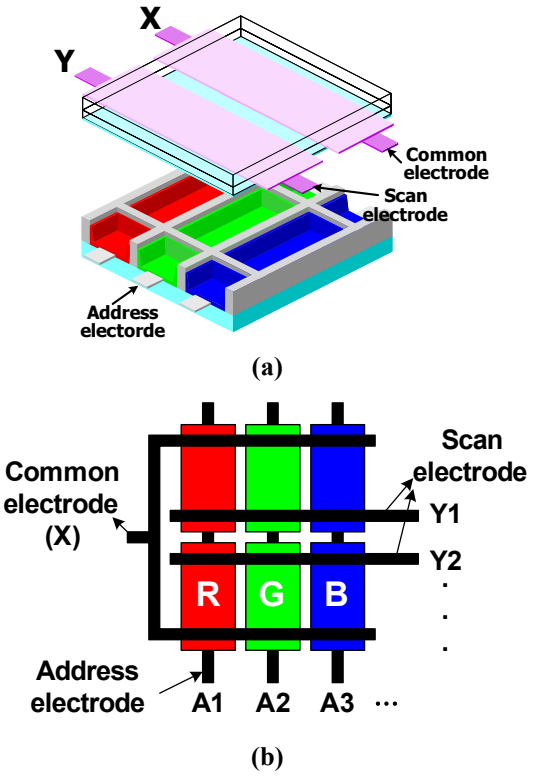

Fig. 1 (a) Test panel structure and (b) schematic diagram of three electrodes in 50-in. full HD panel employed in current study..

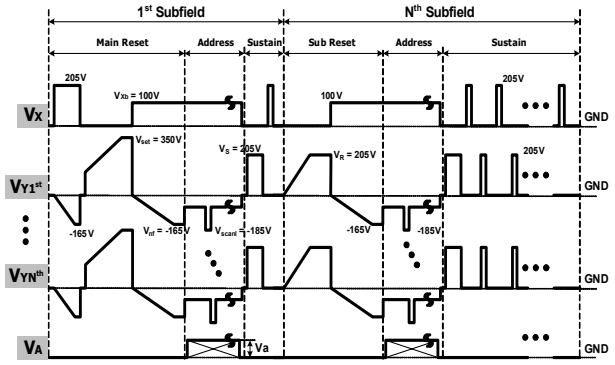

Fig. 2 Driving waveform applied to three electrodes in current study.

common for the R, G, and B cells, implying that the same driving waveforms are applied to the X and Y electrodes except the address (A) electrode for the R, G, and B cells.

Fig. 2 shows the schematic diagram of the driving waveform employed for measuring the address discharge characteristics with main and sub-reset driving waveforms. In 1st subfield of Fig. 2, the rising voltage V_{set}, is 350 V for main reset period and the rising voltage, V_R, is 205 V for sub-reset period. The negative falling voltage, V_{nf} is -165 V for main and sub-reset period.

3. RESULTS AND DISCUSSION

3.1 Address Discharge Characteristics by Reset Driving Waveform

Fig. 3 shows the cell voltage of the measured V_t closed-curve among the R, G, and B cells without initial wall charges. In Fig. 3, V_{tXY} means the discharge start threshold cell voltage between the X and Y electrodes, V_{tAY} means the discharge start threshold cell voltage between the A and Y electrodes, V_{tAX} means the discharge start threshold cell voltage between the A and X electrodes, V_{tYX} means the discharge start threshold cell voltage between the Y and X electrodes, V_{tYA} means the discharge start threshold cell voltage between the Y and A electrodes, and V_{tXA} means the discharge start threshold cell voltage between the X and A electrodes. Table 1 shows the firing voltage of each discharge mode (X-Y, A-Y, A-X, Y-X, Y-A, X-A discharge) at the test panel. As shown in Fig. 3, the cell voltages of the V_t closed-curves were measured among the R, G, and B cells of test panel without initial wall charges.

As shown in Fig. 3 and Table 1, the firing voltages for the X-Y, Y-X discharge (i.e., surface discharge) were observed to be almost the same irrespective of the R, G, and B cells. In the case of the A-Y, A-X discharge (i.e., plate gap discharge under an MgO cathode condition), the firing voltage of the B cell was observed to be higher than that of the R and G cells. For the Y-A, X-A discharge (i.e., plate gap discharge under a phosphor cathode condition), the firing voltage of the G cell was observed to be higher than that of the R and B cells.

Figs. 4 (a) and (b) show the measured V_t closed-curves after the main and sub-reset discharge. As shown in Fig. 4 (a), the V_t closed-curve of the G cell was shifted to the upward direction about by 3 V on the applied voltage plane. This meant that the address discharge delay time of the G cell was slower than that of the other R and B cells. As shown in Fig. 4 (b), the V_t closed-curve of the B cell was shifted to the upward direction (about by 3 V). This meant that the address discharge delay time of the B cell was shower than that of the R and G cells. As a result, Figs. 5 (a) and (b) show the address discharge characteristics after the main and sub reset-periods for the R, G, and B cells. As shown in

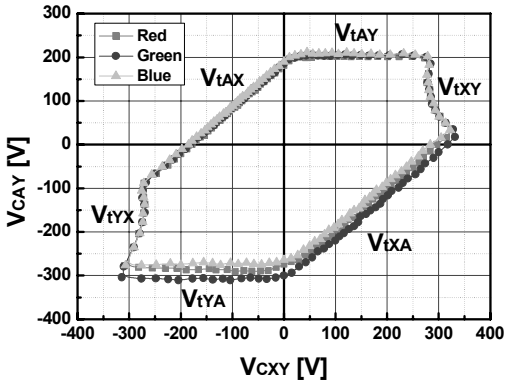

Fig. 3 Measured V_t closed-curves for 50-in. full-HD panel without initial wall charges.

Table 1: Firing voltages measured from R, G, and B cells.

Firing voltage [V]		Red	Green	Blue
MgO Cathode	V_{tXY}	278	278	279
	V_{tAY}	202	205	208
	V_{tAX}	180	183	188
	V_{tYX}	271	270	272
Phosphor Cathode	V_{tYA}	268	307	273
	V_{tXA}	300	318	286

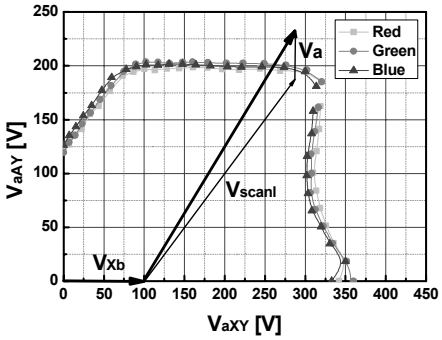

(a) After main reset discharge

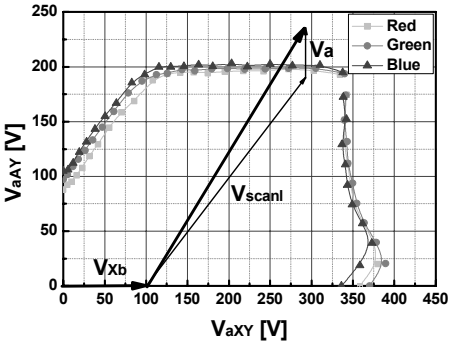

(b) After sub-reset discharge

Fig. 4 Measured V_t closed-curves after main and sub-reset discharges.

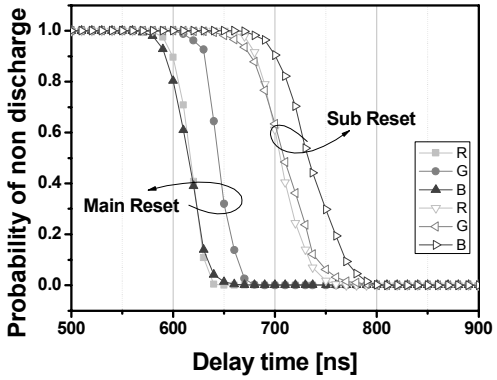

(a)

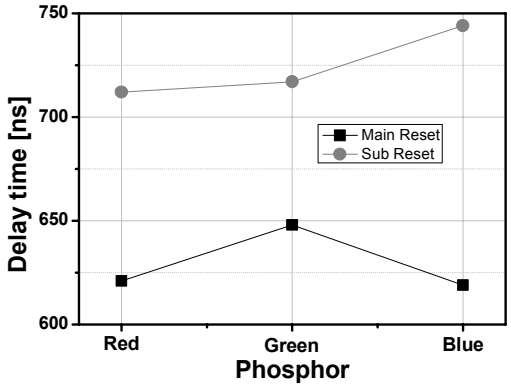

(b)

Fig. 5 (a) Probability of non-discharge and (b) address discharge delay times related to main and sub reset discharges for R, G, and B cells .

Table 2: Various phosphor thicknesses in three test panels, A, B, and C.

	Thickness of Phosphor layers [μm]		
	Panel A	Panel B	Panel C
Red	7.53	8.33	16.26
Green	7.53	10.31	11.5
Blue	9.52	12.69	15.7

Figs. 5 (a) and (b), for the address with main reset, the address discharge delay time was observed to be slowest for the G cell. On the other and, for the address with sub reset, the address discharge delay time was observed to be slowest for the B cell.

3.2 Address Discharge Characteristics by Thickness of Phosphor Layers

The detailed phosphor thicknesses of R, G, and B cells are listed in Table 2.

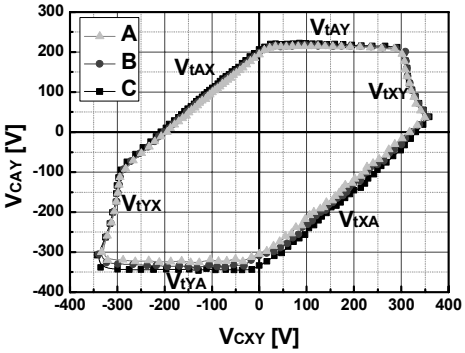

Fig. 6 Measured V_t closed-curves for various thicknesses of red phosphor without initial wall charges.

Table 3: Firing voltages measured in cell with various thicknesses of red phosphor.

Firing voltage [V]		A	B	C
MgO Cathode	V_{tXY}	309	308	310
	V_{tAY}	213	215	219
	V_{tAX}	197	201	208
	V_{tYX}	298	299	301
Phosphor Cathode	V_{tYA}	322	335	344
	V_{tXA}	319	332	346

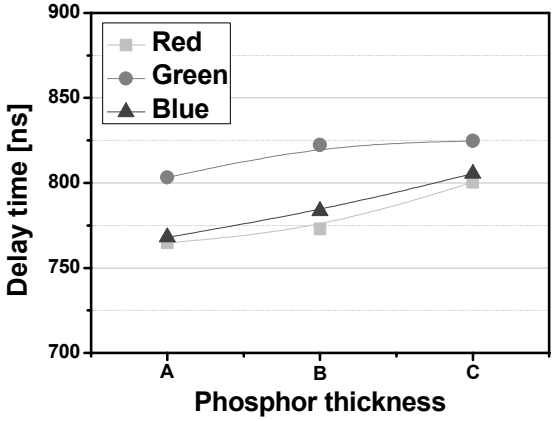

Fig. 7 Measured address discharge delay times according to phosphor thickness in address period.

Fig. 6 shows the measured V_t closed-curves for the various phosphor thicknesses of the R cell without initial wall charges. As shown in Fig. 6, the firing voltage of the plate gap was increased by increasing the phosphor thickness. The A-Y firing voltage and Y-A firing voltage were increased by about 7 V and 20 ~ 30 V, respectively even though the firing voltage of the surface gap was not increased. The detailed firing voltages are listed in Table 3.

Fig. 7 shows the changes in the address discharge delay time relative to the phosphor thicknesses. The ad-

dress discharge delay times were increased by increasing the phosphor thickness because the firing voltage of the plate gap was increased. As shown in Fig. 7, the address discharge delay time of the thinner G phosphor layer was almost the same as that of the thicker R and B phosphor layers. As a result, it is expected that the proper control of the phosphor thickness for R, G, and B cells will contribute to compensating the different address discharge delay phenomena irrespective of the R, G, and B cells.

4. CONCLUSIONS

The address discharge characteristics of ac-PDP strongly depend on the phosphor types. In addition, its address discharge characteristics also depend strongly on the phosphor thickness. Therefore, it is expected that the proper control of the phosphor thickness for R, G, and B cells will compensate the different address discharge delay phenomena irrespective of the phosphor types.

5. REFERENCES

[1] B.-G. Cho, S. I. Lee, and H.-S. Tae, "Modified selective reset waveform to prevent weakness of address discharge characteristics in AC PDP," *IDW'03 Digest* pp.933-936, 2003.

[2] K. Sakita, K. Takayama, K. Awamoto, and Y. Hashimoto, "High-speed address driving waveform analysis using wall voltage transfer function for three terminals and Vt close curve in three-electrode surface-discharge AC-PDPs," *SID'01 Digest*, pp.1022-1025, 2001.

[3] K. Sakita, K. Takayama, K. Awamoto, and Y. Hashimoto, "Ramp setup design technique in three-electrode surface-discharge AC-PDPs," *SID'02 Digest* pp.948-951, 2002.

[4] K. Sakita, K. Takayama, K. Awamoto, and Y. Hashimoto, "Analysis of cell operation at address period using wall voltage transfer function in three-electrode surface-discharge AC-PDPs," *Asia Display/IDW'01 Digest*, pp.841-844, 2001.